Journal of Geophysical Research: Space Physics

RESEARCH ARTICLE
10.1029/2017JA025154

Key Points:
- Solar wind temporal variation regulates the energy flow from the solar wind to the coupled MIT system
- Joule heating in the upper atmosphere depends both on the directly driven processes related to solar wind variability and the intrinsic dynamics of the magnetosphere
- The magnetosphere-ionosphere-thermosphere coupled system has a low-pass filter nature

Correspondence to:
J. Liu,
jingliu@ucar.edu

Citation:
Liu, J., Wang, W., Zhang, B., Huang, C., & Lin, D. (2018). Temporal variation of solar wind in controlling solar wind-magnetosphere-ionosphere energy budget. *Journal of Geophysical Research: Space Physics*, *123*, 5862–5869. https://doi.org/10.1029/2017JA025154

Received 11 JAN 2018
Accepted 26 JUN 2018
Accepted article online 1 JUL 2018
Published online 20 JUL 2018

Temporal Variation of Solar Wind in Controlling Solar Wind-Magnetosphere-Ionosphere Energy Budget

Jing Liu[1], Wenbin Wang[1], Binzheng Zhang[1], Chaosong Huang[2], and Dong Lin[3]

[1]High Altitude Observatory, National Center for Atmospheric Research, Boulder, CO, USA, [2]Air Force Research Laboratory, Kirtland AFB, Albuquerque, NM, USA, [3]Bradley Department of Electrical and Computer Engineering, Virginia Polytechnic Institute and State University, Blacksburg, VA, USA

Abstract Periodic oscillations associated with Alfven waves with periods ranging from several tens of minutes to several hours are commonly seen in the solar wind. It is not yet known how the solar wind oscillation frequency, and thus its temporal variation, regulates the energy flow through the coupled solar wind-magnetosphere-ionosphere-thermosphere system. Utilizing the Coupled Magnetosphere-Ionosphere-Thermosphere Model driven by solar wind and interplanetary magnetic field (IMF), we have analyzed the magnetosphere-ionosphere-thermosphere system response to IMF B_z oscillations with periods of 10, 30, and 60 min from the perspective of energy budget. Our results indicate that the energy flow from the solar wind to geospace depends on the IMF B_z oscillation frequency. The energy coupling efficiency, defined as the ratio of the globally integrated joule heating to Akasofu's Epsilon function, is higher for lower frequency IMF B_z oscillations. Joule heating in the upper atmosphere depends not only on directly driven processes due to solar wind variability but also on the intrinsic dynamics of the magnetosphere (i.e., loading-unloading process). This work highlights the critical role of solar wind and IMF temporal variation and the inductive inertia and resistance of coupled magnetosphere-ionosphere system in controlling the energy transfer in the coupled solar wind-geospace system, which has not been explored before.

1. Introduction

Solar wind energy is dissipated throughout geospace in a number of ways, including ring current dissipation, joule heating, auroral precipitation, and energy deposited in the magnetotail such as plasmoid energy. Joule heating in the auroral and polar regions is the major sink (Koskinen & Tanskanen, 2002; Lu et al., 1998). There are several well-known energy coupling functions that combine different solar wind parameters to estimate the amount of energy transferred from the solar wind into the magnetosphere-ionosphere-thermosphere (MIT) coupled system. One of the most widely used coupling functions is the Epsilon function (Akasofu, 1979), which combines solar wind velocity and the magnitude and clock angle of the interplanetary magnetic field (IMF). The function represents the solar wind Poynting flux transfer into the magnetosphere. Newell et al. (2007) summarized 20 solar wind-magnetosphere coupling functions, which depend on solar wind velocity and number density, or the strength and clock angle of the IMF. None of these studies, however, have taken the solar wind temporal variation into consideration, even though there are a number of studies on the temporal response of the MIT system to changes in the reconnection rate at the magnetopause (e.g., Coroniti & Kennel, 1973; Holzer & Reid, 1975; Lu et al., 2002; Siscoe et al., 2011). This raises a fundamental question: Does the solar wind temporal variation make a difference in the energy coupling efficiency between the solar wind and the coupled magnetosphere-ionosphere system? In particular, what is the total energy input from the solar wind to this coupled system when it is driven by solar wind conditions that oscillate quasi-periodically?

The coupled magnetosphere-ionosphere is a system, which has a significant inductive inertia, capacitance, and resistance. The inductive inertia tends to damp the amplitude of cross polar cap potential relative to trans-magnetosphere boundary potential (Rostoker et al., 1988). The inductive response time of the convection circuit to an oscillation solar wind conditions is several tens of minutes (Rostoker et al., 1988). Solar wind energy flow into this coupled system takes the form of directly driven that release energy immediately and loading unloading processes that part energy is stored. How much directly energy dissipation should depend on how rapidly the Earth's upper atmosphere consumes electromagnetic energy through joule heating, which lies on the ionosphere resistivity.

Quasi-periodic IMF and solar wind velocity oscillations ranging from tens of minutes to a few hours are a signature of Alfven waves in the solar wind, particularly in high-speed streams from coronal holes (e.g., Belcher & Davis Jr., 1971; Kamide et al., 1998). In corotating interaction regions and high-speed stream events, the southward IMF component associated with these oscillations modulates magnetic reconnection, plasma entry into the magnetosphere, and prolonged recovery phases of geomagnetic storms. Events of this type are called "high-intensity, long-duration, continuous AE activity" events (Tsurutanni & Gonzalez, 1987). Presumably, magnetic reconnection between the southward component of the IMF and magnetospheric magnetic fields during these events is the dominant process for the energy transfer from the solar wind to the magnetosphere. Quasiperiodic or pulsed magnetic reconnection in this case may lead to quasiperiodic or pulsed ionospheric convective flows and joule heating, as well as quasiperiodic cusp particle precipitation, polar cap patches, and periodic penetration electric fields in the equatorial ionosphere (e.g., Prikryl et al., 1999; Rae et al., 2004; Rodríguez-Zuluaga et al., 2016; Wei et al., 2008).

The objective of this work is to investigate whether the periodic oscillations in solar wind and IMF have impacts on the energy transfer from the solar wind to the coupled MIT system, how the solar wind oscillation frequency regulates the energy coupling efficiency, and how the MIT system responds to the periodic solar wind driving conditions. We employ the Coupled Magnetosphere-Ionosphere-Thermosphere Model (CMIT; Wang et al., 2004; Wiltberger et al., 2004) to carry out this study. Model description and simulation setup are described in the second section. The analyses of simulation results are performed in the third section, followed by discussion and summary sections.

2. Model Description

The CMIT model is a two-way coupled model between the Lyon-Fedder-Mobarry (LFM) global magnetosphere magnetohydrodynamic code and the Thermosphere-Ionosphere-Electrodynamics General Circulation Model (TIEGCM) via the Magnetosphere-Ionosphere Coupler/Solver module (Merkin & Lyon, 2010). LFM is an ideal magnetohydrodynamic solver for the three-dimensional solar wind-magnetosphere interaction system (Lyon et al., 2004). TIEGCM is an ionosphere-thermosphere coupled model that solves the three-dimensional, energy, momentum, and continuity equations for both neutrals and ions (Roble et al., 1988). This detailed coupling scheme between LFM, TIEGCM, and Magnetosphere-Ionosphere Coupler/Solver has been documented in Wiltberger et al. (2004) and Wang et al. (2004).

This simulation is driven by idealized solar wind, IMF, and solar minimum conditions with solar wind density N_{SW} = 5 cm^{-3}, speed V_{SW} = 500 km/s, IMF$|B|$ = 10 nT, and $F_{10.7}$ = 77. In this model setup, the solar wind is defined in the GSM coordinates. The solar wind speed in the y and z directions is zero ($V_y = V_z = 0$), and IMF x and z components are also set to zero ($B_x = B_y = 0$). The CMIT model is driven by the IMF B_z = 0 nT condition for 4 hr as an initial state and then by sinusoidally oscillating IMF B_z between −10 and +10 nT, with different periods of 10, 30, and 60 min, respectively (Figure 1a). Furthermore, all numerical simulations are performed for the December Solstice condition when the upper atmosphere joule heating shows hemisphere asymmetry.

3. Result Analysis

Figure 1 shows the time series of IMF B_z, the Epsilon function, and joule heating from CMIT for different IMF B_z oscillation periods during the first 2 hr of model simulations. IMF B_z oscillations with 10-, 30-, and 60-min periods are color coded in black, blue, and red lines, respectively. The Epsilon function (ε), which is usually used to represent the energy transfer from the solar wind to the magnetosphere, is calculated based on the following equation (Akasofu, 1979):

$$\varepsilon(W) = \frac{4\pi}{\mu_0} vB^2 \sin^4\left(\frac{\theta}{2}\right) l_0^2.$$

These variables v, B, θ, and l_0 are the solar wind velocity, the intensity of the solar wind magnetic field, the IMF clock angle, and the scaling factor. The factor l_0 is an "effective cross-sectional area" of the magnetosphere determined empirically to be l_0 = 7 RE (Perreault & Akasofu, 1978). Southward IMF B_z switches on the

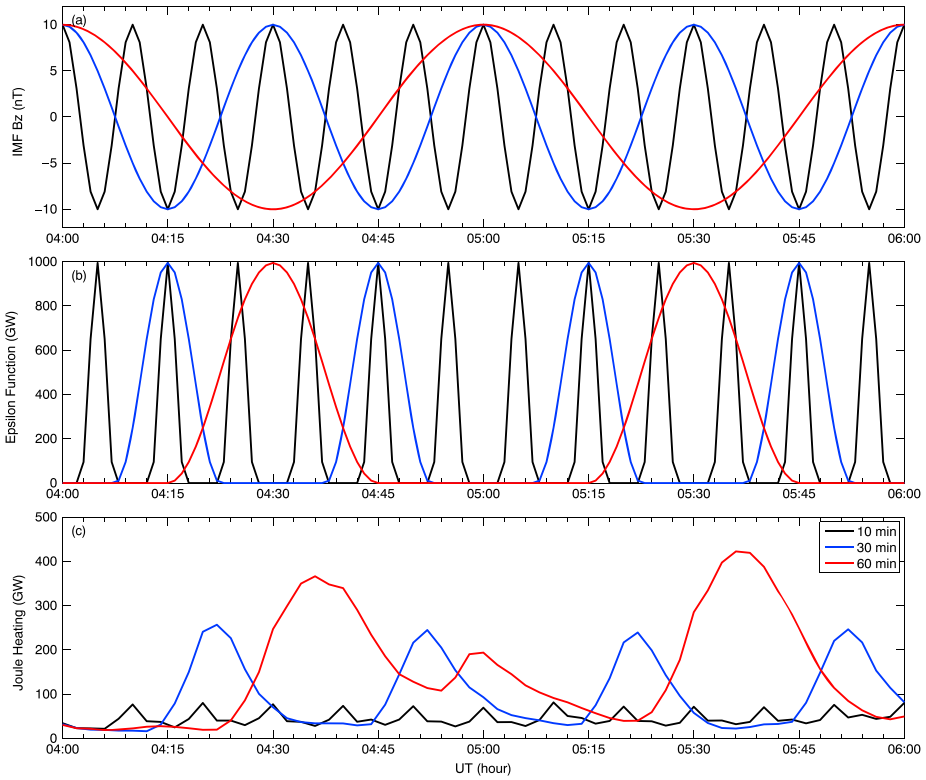

Figure 1. Interplanetary magnetic field (IMF) B_z, Epsilon function, and joule heating variabilities for different periods. IMF B_z oscillating with 10, 30, and 60 min are colored black, blue, and red lines, respectively.

energy input, whereas northward IMF B_z switches it off. Total global integrated joule heating is calculated by summing from 40° geographic latitudes to the poles for both hemispheres.

As shown in Figures 1a and 1b and described by the equation, it is not surprising to see that the ε function acts as a half wave rectifier to regulate solar wind energy transfer into the magnetosphere. In other words, to the first-order approximation, energy transfer from the solar wind to the magnetosphere occurs when IMF B_z has a southward component. The amplitude of the ε function does not change with IMF B_z oscillation frequency. The total energy into the magnetosphere is the same for all three cases in 1-hr period, which is 8.95×10^{14} J calculated from ε function. However, the CMIT-calculated joule heating depends greatly on the oscillation frequency.

Siscoe et al. (2011) discussed the difference of ionospheric convection when IMF changes from northward to southward and vise versa. They also showed that ionospheric convection during the transient period of IMF could be significantly different from that under persistent IMF conditions. Our study is consistent with their results in the general sense that when studying the coupling between the solar wind and the magnetosphere, the temporal variation of the solar wind must be taken into account, both for ionospheric convection configuration discussed in Siscoe et al. (2011) and energy transfer rate from the solar wind to the magnetosphere ionosphere system studied in this paper. As shown in Figure 1c, joule heating tends to be stronger when IMF B_z is southward for a longer period of time. The peak energy deposition in the upper atmosphere evidently increases with an increase in the duration of southward IMF. The peak power amplitudes of joule heating are ~400, ~280, and ~80 GW for solar wind with oscillations at periods of 60, 30, and 10 min, respectively. The total globally integrated energy depositions from joule heating during 0400–0500 UT are 4.94×10^{14}, 3.47×10^{14}, 1.55×10^{14} J for the three cases of solar wind conditions. Thus, the coupling efficiencies of the total energy deposition in the upper atmosphere, relative to that estimated by the ε function, are 55.2%, 38.8%, and 17.3% for 60-, 30-, and 10-min solar wind oscillations, respectively. Another interesting feature is that joule heating for the 60-min IMF B_z oscillation has an additional peak that is about half as large as

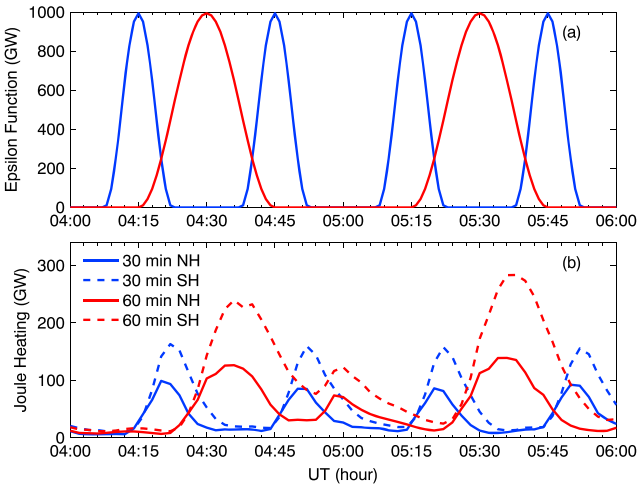

Figure 2. Variations of (top) ε parameter (top panel) and (bottom) hemisphere-integrated joule heating. Joule heating from Southern Hemisphere and Northern Hemisphere are indicated by dashed and solid lines, respectively.

the major one. These secondary peaks occur in both hemispheres for 60-min oscillations of solar wind, but they disappear for cases of 30- and 10-min periods.

In order to acquire a better understanding of the relative contribution to the global integrated joule heating from each hemisphere, we show in Figure 2 the ε function (top) and joule heating in each hemisphere (bottom) for the 30- and 60-min solar wind cases. The ε parameter serves as a reference for the energy input into the magnetosphere. Joule heating in the summer (southern) hemisphere is nearly twice as large as that in the winter (northern) hemisphere. This difference is related to the fact that Pedersen conductivity is about 2.5 times higher in the summer hemisphere than in the winter hemisphere due to stronger solar illumination, while cross polar cap potential is generally weaker in the summer hemisphere compared to the winter hemisphere. This implies that the driver acts more like a voltage source. Another noteworthy feature is that hemisphere-integrated joule heating lags behind ε by 10 min or so, varying with solar wind oscillation period. This time delay between IMF changes near the magnetopause and initial ionosphere response accords well with previous simulations or observations results (e.g., Lu et al., 2002; Ridley et al., 1998; Ruohoniemi & Greenwald, 1998).

The total amount of open magnetic flux inside the magnetosphere is an important factor in controlling the magnetospheric state and is determined by dayside and nightside merging rates (Siscoe & Huang, 1985). Dayside magnetic reconnection is directly driven by the upstream solar wind and is regulated by the magnitude and the clock angle of the IMF. The physical process associated with nightside reconnection, for example, the substorm phenomena, has yet to be fully resolved. In the global magnetosphere simulation, when the oscillatory IMF switches from northward to southward, isolated substorms are generated in the simulations through the magnetic flux loading-unloading process, which is a consequence of a significant imbalance between dayside reconnection rate and nightside reconnection rate (Gordeev et al., 2017). In order to know the cause of the secondary peaks of joule heating appearing in Figures 1 and 2, Figure 3 illustrates open flux and its gradient. The open flux is calculated by identifying the open and closed magnetic field line boundary in the polar ionosphere via tracing the magnetic field lines. To the first order, open flux is strongly modulated by IMF B_z; that is, open flux attains its maximum at the point when IMF B_z starts to turn from southward to northward. But for the 60-min period, we see a strong dip in the flux gradient at around 04:57 UT, which is associated with substorm activity. After accumulating a significant amount of open magnetic flux (>0.6 GWb) in the lobe due to the southward IMF driving, an isolated substorm occurs in the simulation and results in a dramatic decrease in open flux. In the 30-min period simulation, the accumulated open magnetic flux was always below 0.5 GWb and no isolated substorms occurred during the simulation, indicating that the imbalance between the dayside and nightside reconnection is not enough to initiate substorm-like activity in order to release the open flux. This agrees with Milan et al. (2007) that the average magnetosphere magnetic flux content during 25 tail reconnection events at onset is 0.65 GWb and these tail reconnection events seldom occur under 0.35 GWb.

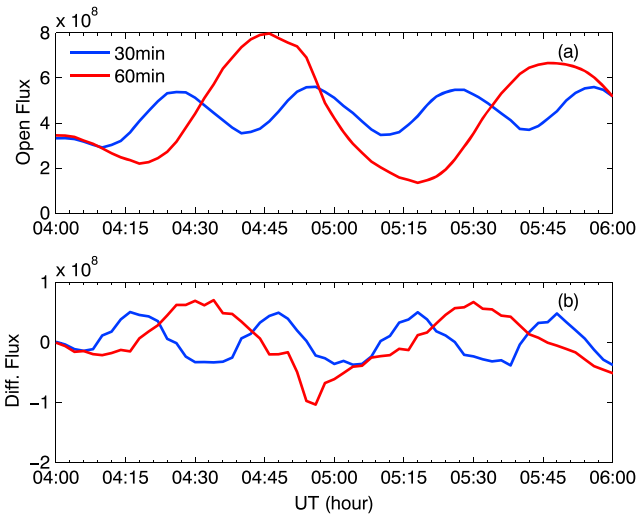

Figure 3. Variations of magnetosphere open flux (in units of Wb) and its gradient.

Figure 4 presents the cross correlation between joule heating and the Epsilon function. Joule heating is calculated from the electric field ($\sigma_p E^2$). Neutral wind effects have been included into TIEGCM, which is a self-consistent mode solving ion and neutral momentum equations, as well as electrodynamo. TIEGCM model, which is the ionosphere-thermosphere part of CMIT, is not equal area grid. We calculated area-weighted joule heating in each horizontal grid and then integrate them in the vertical direction with 10-km grid resolution. The top panel shows that globally integrated joule heating generally lags behind the ε parameter by

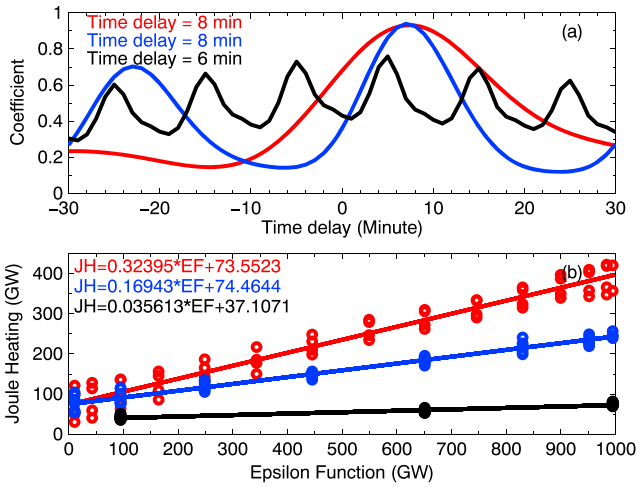

Figure 4. Cross correlation between joule heating and the Epsilon function. (top) Time delay and the correlation coefficient between joule heating and the Epsilon function. (bottom) Scatterplots of joule heating versus the Epsilon function for different periods. The solid lines show the trend of the linear regression.

6–8 min. This time delay is in general agreement with the results from Lu et al. (2002), in which they showed that there is a 7-min time delay between the IMF southward turning and initial ionosphere response. The black, blue, and red lines indicate the IMF oscillations at 10, 30, and 60 min, respectively. The time delay between them has been taken into consideration in the linear regression. The slope of linear regression in the bottom panel denotes the energy coupling efficiency from the solar wind into the upper atmosphere. Coupling efficiency tends to increase with solar wind oscillation period. For instance, coupling efficiencies are 0.036, 0.17, and 0.32 for 10-, 30-, and 60-min periods, respectively. This reinforces the importance of solar wind temporal variation in controlling the energy coupling between the solar wind and the magnetosphere and the total energy deposition into the upper atmosphere.

4. Discussion

The solar wind energy transferred into the magnetosphere takes the form of joule heating, particle precipitation, ring current injection, and plasmoid ejection in the tail. In order to formulate this solar wind energy partition, different coupling functions are constructed in combination with different solar wind parameters such as solar wind velocity, B_z, and B_y (e.g., Akasofu, 1979; Newell et al., 2007). Apparently, the magnitudes of these solar wind parameters have significant effects on the energy coupling efficiency. Our research also reinforces the importance of solar wind temporal variation in regulating energy transfer in the solar wind-geospace coupled system.

Two physical processes are important in transferring solar wind energy into the upper atmosphere. One is dayside reconnection between solar wind and magnetospheric plasmas, in which solar wind energy has a direct dissipation in the upper atmosphere. As shown in Figure 4, it takes 6–8 min for this energy dissipation process to occur, which is a consequence of the finite inductance of the MIT system (Holzer & Reid, 1975; Siscoe et al., 2011). The other is nightside reconnection in which solar wind energy accumulates in the magnetotail and then is suddenly released to the Earth's upper atmosphere, triggered either by solar wind variability or by magnetosphere internal processes. For example, in Figure 1, joule heating for the 60-min period case has another peak in the declining phase of joule heating. Joule heating by the "driven process" is larger than that by the "loading-unloading" process. In Figure 1, a substorm occurs only for the 60-min IMF B_z oscillation and leads to periodic magnetotail energy release into the ionosphere. This finding agrees with the results from Blanchard and McPherron (1995) in which auroral ionospheric currents' response to solar wind driving for individual substorms is composed by a low-pass filter responsible for the ionospheric electric fields due to the reconnection fields and a filter composed of a delayed delta function caused by the magnetotail substorm.

Why do we see substorms only for the 60-min period IMF B_z oscillation? Substorm is a phenomenon that is global magnetosphere reconfiguration, which involves Earth's magnetotail dynamics, solar wind energy storage, and release. Its triggering mechanisms are not fully understood and could be associated with a near-Earth dipolarization process or with magnetic reconnection at ~20 to 30 R_E. Even though disputes exist in the substorm triggering mechanism, there is rather general agreement that the magnetosphere exhibits a growth phase and requires energy and magnetic flux storage in the magnetotail prior to substorm onset. CMIT is capable of capturing substorm behavior, and this substorm-related initial buildup process takes about 50 min in the LFM model (Gordeev et al., 2017). If the IMF B_z oscillation between northward and southward is too fast, the loading-unloading cycle is not completed. Thus, less energy and magnetic flux are stored in the nightside magnetotail, reducing the chance of the occurrence of substorm.

Figure 4 shows that the energy coupling efficiency from the solar wind driver to the upper atmosphere depends on the solar wind oscillation frequency or, in general, the temporal variation of the solar wind and IMF B_z; that is, the energy coupling efficiency tends to be higher for lower frequency IMF B_z oscillations or slow varying solar winds conditions. Why is the energy coupling efficiency higher for lower frequency IMF B_z oscillations? The energy transfer from the solar wind to the magnetosphere is caused by magnetic

reconnection between IMF and Earth's magnetic field (Dungey, 1961). The global rate is determined by the product of the merging line length and the rate at which closed magnetic flux at the magnetopause merges with the magnetosheath magnetic field. The reconnection rate is $R \approx 0.1\ v_A B$ at the dayside magnetopause, where v_A and B are the Alfvén speed and magnetic field intensity in the reconnection inflow region. It takes several minutes for the southward solar wind IMF to propagate from the bow shock to the magnetopause, and another minute or so for information to propagate to the ionosphere that merged convecting flux tubes at the magnetopause that will drive plasma flows there (e.g., Ruohoniemi & Greenwald, 1998). In this case, if IMF B_z varies too fast, the magnetic flux accumulation at the magnetopause is diminished, and the dayside magnetopause reconnection cannot achieve the peak energy transfer state and thus less energy flux is delivered into magnetosphere.

Presumably, a long duration of southward IMF B_z allows for continuous energy and momentum transfer from the solar wind into the magnetosphere through magnetic reconnection. As IMF B_z changes from southward to northward, it takes time for the magnetosphere to achieve a steady state. Here we can make a rough estimation of the time delay between dayside magnetopause reconnection and nightside magnetotail reconnection. The delay is calculated by estimating the propagation time of open flux tubes to travel between these two reconnection points. The distance between the magnetopause (~8 R_E on the dayside) and the magnetotail neutral line (50–100 R_E on the nightside) is about 58–108 R_E. Assuming that solar wind speed is 500 km/s, and the transit time for the open flux tube to propagate from the dayside to the nightside is about 12–23 min, which agrees with previous calculations (Cowley & Lockwood, 1992; Murr & Hughes, 2001). In addition, the reconfiguration time, which is the time required for the coupled magnetosphere-ionosphere system to reconfigure itself into a new stable state, should also be taken into account. It takes about 5–10 min for noon high-latitude ionosphere in response to sharp IMF turnings and longer for other local times away from noon (Murr & Hughes, 2001). To add up, it takes about 17–32 min to complete the dayside-to-nightside open magnetic flux propagation and energy transfer. If the change of solar wind is too fast, nightside reconnection will barely engage and will reconnect little magnetic flux if IMF B_z varies too fast and changes its orientation. Thus, less energy will be stored and dissipated on the nightside. Therefore, less energy is dissipated in the upper atmosphere through the joule heating process on both the dayside and nightside, for the case of high frequency IMF B_z oscillations as shown in Figure 1.

If the IMF B_z changes fast, the magnetosphere is in a mixed state with both northward and southward IMF B_z driving conditions. They are more likely to cancel out each other, reducing the coupling efficiency between the solar wind-magnetosphere and ionosphere-thermosphere system, and thus, cross polar cap potential, field-aligned currents, and hemispheric power are also reduced (e.g., Pham et al., 2016). In addition, the filed-aligned current system associated with magnetosphere-ionosphere coupling has an appreciable inductive inertia which damps the CPCP amplitude relative to reconnection potential, and this attenuation efficiency depends on solar wind oscillation frequency (Sanchez et al., 1991).

Coupling functions in describing the solar wind-magnetosphere-ionosphere combine the instantaneous solar wind parameters without taking the historic temporal solar wind variation into account that cannot precisely describe instantaneous solar wind-magnetosphere-ionosphere interactions. The ionosphere-thermosphere coupled system has an even longer memory compared with the magnetosphere (Liu et al., 2010). Thus preexisting solar wind condition that determines current magnetosphere-ionosphere status also has important implication in the current step.

5. Conclusion

In order to understand energy coupling between the solar wind and the magnetosphere, and energy deposition from the magnetosphere and solar wind into the thermosphere and ionosphere, when solar wind and IMF has strong temporal variations, a set of CMIT numerical simulations have been performed. A number of new and interesting results are obtained from these simulations. The energy coupling efficiency for the solar wind energy flow into thermosphere and ionosphere, in the form of joule heating, tends to be higher for low-frequency IMF B_z oscillations. The coupling efficiencies of peak power are 0.036, 0.17, and 0.32, while the total energy transfer efficiencies are 17.3%, 38.8%, 55.2% for IMF B_z oscillations with 10, 30, and 60-min periods, respectively. Storm-time joule heating is not only determined by directly driven solar wind process but it also exhibits "loading-unloading" dynamics for the 60-min IMF oscillations, even though the direct

driving dominates. In addition, hemispheric integrated joule heating is hemispherically asymmetric and larger in the summer hemisphere.

Acknowledgments
This research is supported by NASA grants NNX14AE06G, NNX15AB83G, NNX17A142G, and 80NSSC17K0013. We would like to acknowledge Bill Lotko for his helpful discussion. The simulation data are archived in the NCAR supercomputer and can be accessible upon request (jingliu@ucar.edu).

References

Akasofu, S.-I. (1979). Interplanetary energy flux associated with magnetospheric substorms. *Planetary and Space Science*, *27*(4), 425–431. https://doi.org/10.1016/0032-0633(79)90119-3

Belcher, J. W., & Davis, L. Jr. (1971). Large amplitude Alfven waves in the interplanetary medium. *Journal of Geophysical Research*, *76*(16), 3534–3563. https://doi.org/10.1029/JA076i016p03534

Blanchard, G. T., & McPherron, R. L. (1995). Analysis of the linear response function relating AL to VBs for individual substorms. *Journal of Geophysical Research*, *100*(A10), 19,155–19,165. https://doi.org/10.1029/95JA01341

Coroniti, F. V., & Kennel, C. F. (1973). Can the ionosphere regulate magnetospheric convection? *Journal of Geophysical Research*, *78*(16), 2837–2851. https://doi.org/10.1029/JA078i016p02837

Cowley, S. W. H., & Lockwood, M. (1992). Excitation and decay of solar wind-driven flows in the magnetosphere-ionosphere system. *Annales de Geophysique*, *10*, 103–115.

Dungey, J. W. (1961). Interplanetary magnetic field and the auroral zones. *Physical Review Letters*, *6*(2), 47–48. https://doi.org/10.1103/PhysRevLett.6.47

Gordeev, E., Sergeev, V., Tsyganenko, N., Kuznetsova, M., Rast, L., et al. (2017). The substorm cycle as reproduced by global MHD models. *Space Weather*, *15*, 131–149. https://doi.org/10.1002/2016SW001495

Holzer, T. E., & Reid, G. C. (1975). The response of the dayside magnetosphere-ionosphere system to time-varying field line reconnection at the magnetopause, 1. Theoretical model. *Journal of Geophysical Research*, *80*(16), 2041–2049. https://doi.org/10.1029/ja080i016p02041

Kamide, Y., Baumjohann, W., Daglis, I. A., Gonzalez, W. D., Grande, M., Joselyn, J. A., et al. (1998). Current understanding of magnetic storms: Storm-substorm relationships. *Journal of Geophysical Research*, *103*(A8), 17,705–17,728. https://doi.org/10.1029/98JA01426

Koskinen, H. E. J., & Tanskanen, E. (2002). Magnetospheric energy budget and the epsilon parameter. *Journal of Geophysical Research*, *107*(A11), 1415. https://doi.org/10.1029/2002JA009283

Liu, J., Zhao, B., & Liu, L. (2010). Time delay and duration of ionospheric total electron content responses to geomagnetic disturbances. *Annales de Geophysique*, *28*(3), 795–805. https://doi.org/10.5194/angeo-28-795-2010

Lu, G., Baker, D. N., McPherron, R. L., Farrugia, C. J., Lummerzheim, D., Ruohoniemi, J. M., et al. (1998). Global energy deposition during the January 1997 magnetic cloud event. *Journal of Geophysical Research*, *103*(A6), 11,685–11,694. https://doi.org/10.1029/98JA00897

Lu, G., Holzer, T. E., Lummerzheim, D., Ruohoniemi, J. M., Stauning, P., Troshichev, O., et al. (2002). Ionospheric response to the interplanetary magnetic field southward turning: Fast onset and slow reconfiguration. *Journal of Geophysical Research*, *107*(A8), 1153. https://doi.org/10.1029/2001JA000324

Lyon, J., Fedder, J., & Mobarry, C. (2004). The Lyon-Fedder-Mobarry (LFM) global MHD magnetospheric simulation code. *Journal of Atmospheric and Solar - Terrestrial Physics*, *66*(15–16), 1333–1350. https://doi.org/10.1016/j.jastp.2004.03.020

Merkin, V. G., & Lyon, J. G. (2010). Effects of the low-latitude ionospheric boundary condition on the global magnetosphere. *Journal of Geophysical Research*, *115*, A10202. https://doi.org/10.1029/2010JA015461

Milan, S. E., Provan, G., & Hubert, B. (2007). Magnetic flux transport in the Dungey cycle: A survey of dayside and nightside reconnection rates. *Journal of Geophysical Research*, *112*, A01209. https://doi.org/10.1029/2006JA011642

Murr, D. L., & Hughes, W. J. (2001). Reconfiguration timescales of ionospheric convection. *Geophysical Research Letters*, *28*(11), 2145–2148. https://doi.org/10.1029/2000GL012765

Newell, P. T., Sotirelis, T., Liou, K., Meng, C.-I., & Rich, F. J. (2007). A nearly universal solar wind-magnetosphere coupling function inferred from 10 magnetospheric state variables. *Journal of Geophysical Research*, *112*, A01206. https://doi.org/10.1029/2006JA012015

Perreault, P., & Akasofu, S. I. (1978). A study of geomagnetic storms. *Geophysical Journal of the Royal Astronomical Society*, *54*(3), 547–573. https://doi.org/10.1111/j.1365-246X.1978.tb05494.x

Pham, K. H., Lopez, R. E., & Bruntz, R. (2016). The effect of a brief northward turning in IMF Bz on solar wind magnetosphere coupling in a global MHD simulation. *Journal of Geophysical Research: Space Physics*, *121*, 4291–4299. https://doi.org/10.1002/2015JA021982

Prikryl, P., MacDougall, J. W., Grant, I. F., Steele, D. P., Sofko, G. J., & Greenwald, R. A. (1999). Observations of polar patches generated by solar wind Alfven wave coupling to the dayside magnetosphere. *Annales de Geophysique*, *17*(4), 463–489. https://doi.org/10.1007/s00585-999-0463-0

Rae, I. J., Fenrich, F. R., Lester, M., McWilliams, K. A., & Scudder, J. D. (2004). Solar wind modulation of cusp particle signatures and their associated ionospheric flows. *Journal of Geophysical Research*, *109*, A03223. https://doi.org/10.1029/2003JA010188

Ridley, A. J., Clauer, C. R., Lu, G., & Papitashvili, V. O. (1998). A statistical study of the ionospheric convection response to changing interplanetary magnetic field conditions using the assimilative mapping of ionospheric electrodynamics technique. *Journal of Geophysical Research*, *103*(A3), 4023–4039. https://doi.org/10.1029/97JA03328

Roble, R. G., Ridley, E. C., & Richmond, A. D. (1988). A coupled thermosphere/ionosphere general circulation model. *Geophysical Research Letters*, *15*(12), 1325–1328. https://doi.org/10.1029/GL015i012p01325

Rodríguez-Zuluaga, J., Radicella, S. M., Nava, B., Amory-Mazaudier, C., Mora-Páez, H., & Alazo-Cuartas, K. (2016). Distinct responses of the low-latitude ionosphere to CME and HSSWS: The role of the IMF Bz oscillation frequency. *Journal of Geophysical Research: Space Physics*, *121*, 11,528–11,548. https://doi.org/10.1002/2016JA022539

Rostoker, G., Savoie, D., & Phan, T. D. (1988). Response of magnetosphere-ionosphere current systems to changes in the interplanetary magnetic field. *Journal of Geophysical Research*, *93*(A8), 8633. https://doi.org/10.1029/JA093iA08p08633

Ruohoniemi, J. M., & Greenwald, R. A. (1998). The response of high-latitude convection to a sudden southward IMF turning. *Geophysical Research Letters*, *25*(15), 2913–2916. https://doi.org/10.1029/98GL02212

Sanchez, E. R., Siscoe, G. L., & Meng, C.-I. (1991). Inductive attenuation of the transpolar voltage. *Geophysical Research Letters*, *18*(7), 1173–1176. https://doi.org/10.1029/91GL01155

Siscoe, G. L., Farrugia, C. J., & Sandholt, P. E. (2011). Comparison between the two basic modes of magnetospheric convection. *Journal of Geophysical Research*, *116*, A05210. https://doi.org/10.1029/2010JA015842

Siscoe, G. L., & Huang, T. S. (1985). Polar cap inflation and deflation. *Journal of Geophysical Research*, *90*(A1), 543–547. https://doi.org/10.1029/JA090iA01p00543

Tsurutanni, B. T., & Gonzalez, W. D. (1987). The cause of high-intensity long duration continuous AE activity (HILDCAAS): Interplanetary Alfven wave trains. *Planetary and Space Science*, *35*(4), 405–412. https://doi.org/10.1016/0032-0633(87)90097-3

Wang, W., Wiltberger, M., Burns, A. G., Solomon, S. C., Killeen, T. L., Maruyama, N., & Lyon, J. G. (2004). Initial results from the Coupled Magnetosphere-Ionosphere-Thermosphere Model: Thermosphere-ionosphere responses. *Journal of Atmospheric and Solar - Terrestrial Physics*, *66*(15–16), 1425–1441. https://doi.org/10.1016/j.jastp.2004.04.008

Wei, Y., Hong, M., Wan, W., Du, A., Lei, J., Zhao, B., et al. (2008). Unusually long lasting multiple penetration of interplanetary electric field to equatorial ionosphere under oscillating IMF Bz. *Geophysical Research Letters*, *35*, L02102. https://doi.org/10.1029/2007GL032305

Wiltberger, M., Wang, W., Burns, A. G., Solomon, S. C., Lyon, J. G., & Goodrich, C. C. (2004). Initial results from the coupled magnetosphere ionosphere thermosphere model: Magnetospheric and ionospheric responses. *Journal of Atmospheric and Solar - Terrestrial Physics*, *66*(15–16), 1411–1423. https://doi.org/10.1016/j.jastp.2004.03.026